Real-Time Refinement of Subthalamic Nucleus Targeting Using Bayesian Decision-Making on the Root Mean Square Measure

Anan Moran, BSc,[1]* Izhar Bar-Gad, PhD,[1] Hagai Bergman, MD, PhD,[2] and Zvi Israel, MD[3]

[1]*Gonda Multidisciplinary Brain Research Center and Faculty of Life Sciences, Bar Ilan University, Ramat Gan, Israel*
[2]*Department of Physiology, Hadassah Medical School and Interdisciplinary Center for Neural Computation, Hebrew University, Jerusalem, Israel*
[3]*Department of Neurosurgery, Hadassah University Hospital, Jerusalem, Israel*

Abstract: The subthalamic nucleus (STN) is a major target for treatment of advanced Parkinson's disease patients undergoing deep brain stimulation surgery. Microelectrode recording (MER) is used in many cases to identify the target nucleus. A real-time procedure for identifying the entry and exit points of the STN would improve the outcome of this targeting procedure. We used the normalized root mean square (NRMS) of a short (5 seconds) MER sampled signal and the estimated anatomical distance to target (EDT) as the basis for this procedure. Electrode tip location was defined intraoperatively by an expert neurophysiologist to be before, within, or after the STN. Data from 46 trajectories of 27 patients were used to calculate the Bayesian posterior probability of being in each of these locations, given RMS-EDT pair values. We tested our predictions on each trajectory using a bootstrapping technique, with the rest of the trajectories serving as a training set and found the error in predicting the STN entry to be (mean ± SD) 0.18 ± 0.84, and 0.50 ± 0.59 mm for STN exit point, which yields a 0.30 ± 0.28 mm deviation from the expert's target center. The simplicity and computational ease of RMS calculation, its spike sorting-independent nature and tolerance to electrode parameters of this Bayesian predictor, can lead directly to the development of a fully automated intraoperative physiological procedure for the refinement of imaging estimates of STN borders. © 2006 Movement Disorder Society

Key words: Parkinson's disease; deep brain stimulation; Bayesian inference; root mean square; microelectrode recording; target localization

Deep brain stimulation (DBS) surgery is routinely performed on patients with severe Parkinson's disease (PD).[1–3] During surgery, macroelectrodes are stereotactically implanted in specific nuclei, typically the subthalamic nucleus (STN)[3] (but see Anderson and colleagues[4] for other targets) for the purpose of delivering chronic high-frequency stimulation. Success of the surgery is largely dependent on identifying the exact location of this small target nucleus. The precise location of the electrode contacts ensures optimal results with minimum side effects.[3] In many medical centers, the target location is confirmed and refined intraoperatively by a neurophys-iologist using extracellular microelectrode recording (MER).[5,6] The observed neurophysiological parameters may include background noise level, firing rate, firing pattern, spike shape, and local field potential (LFP) spectrum.[7–9] The evaluation of some of these parameters requires special neurophysiological expertise, is sensitive to human error, and often takes a long time. Furthermore, recorded parameters are also sensitive to the electrode configuration, such as tip geometry and impedance. Previous work has attempted to construct dedicated tools for brain structure recognition,[10] present parameters in an appealing manner for the surgical team,[11] and define a quality index for the trajectory.[12] Although all these parameters provide useful information for identifying the STN, their value distributions overlap with the values of locations outside the STN, and the actual decision on the location is still left to the surgical team.

Our aim was to generate a robust procedure for STN localization that will advise the surgical team intraoper-

*Correspondence to: Dr. Anan Moran, Gonda Multidisciplinary Brain Research Center, Bar Ilan University, Ramat-Gan, Israel.
E-mail: ananmo@gmail.com

atively, in real-time, of the electrode position. We used a Bayesian inference system based on two parameters: estimated distance to target (EDT), measured from a predicted center of target point that is calculated using imaging data in a preoperative phase, and normalized root mean square (NRMS) of the electrical signal recorded by the electrode. The recommendation made by the system was evaluated relative to decisions made by an expert neurophysiologist intraoperatively. The evaluation of the system performance indicated promising results in identifying and refining STN borders. There are three main advantages to this method: it does not rely on spike detection and sorting procedures, only a short signal recording is required, and it is unaffected by variability in electrode properties. This tool can be easily integrated into ongoing intraoperative guiding applications and thus assist the surgical team in STN localization.

PATIENTS AND METHODS

All surgical patients met accepted selection criteria for STN DBS and signed informed consent for surgery with MER. Surgery was performed using the CRW stereotactic frame (Radionics, Burlington, MA). STN target coordinates were chosen as a composite of AC-PC–based location and MRI using Framelink software (Medtronic, Minneapolis, MN). A single pass using one or two microelectrodes was made starting from 10 mm above the calculated target. Further passes were only made if the results of microrecording and macrostimulation were suboptimal in the first pass. The trajectories used in this study were only the ones with a STN width over 3 mm.

Data Acquisition and Analysis

Data acquisition was conducted with the MicroGuide system (AlphaOmega Engineering, Nazareth, Israel). Neurophysiological activity was recorded via polyimide-coated tungsten microelectrodes (Frederick Haer, Bowdoinham, ME; impedance = 0.48 ± 0.17 MΩ; range, 0.19–0.9 MΩ; measured at 1 KHz, at the beginning of each trajectory). The distance between two microelectrodes when used simultaneously in a track was 2 mm. The recorded signal was amplified by 10,000 and bandpassed between 250 to 6,000 Hz using a four-pole Butterworth filter. The signal was sampled at 24 KHz, by 12 bit A/D converter, using a ±5 V input range (i.e., ~0.25 μV amplitude resolution). Following a 2-second signal stabilization period after electrode movement cessation, the next 5 seconds were recorded. Shorter recordings were rejected. The microelectrode was advanced in steps ranging from 0.05 to 0.3 mm, typically using shorter steps closer to the presumed location of the STN. All the

statistics presented in this article use mean ± standard deviation notation.

STN entry and exit points were marked intraoperatively by an expert neurophysiologist who attended all operations and was blinded to the system recommendations. His decisions were considered the gold standard for the learning system and had divided the recorded sessions to three location groups: pre, within, and post-STN.

Parameters of Interest

The need for real-time computation feasibility was a crucial guideline when choosing the parameters to work with. Therefore, we decided not to use parameters that resulted from procedures for the discrimination of single units. This was done despite the many studies describing STN spike-related information such as firing rate, oscillations, and burstiness[2,13–15] due to the computational difficulty and susceptibility to errors of these procedures,[16] especially when performed in real time. Instead, we used the root mean square (RMS) value of the sampled signal recorded by the electrode, measured in volts, as the main parameter for evaluating electrode position. RMS is defined as follows (Eq. 1):

$$\text{RMS}(\vec{X}) = \sqrt{\frac{\sum_{i=1}^{n} X_i^2}{n}} \tag{1}$$

where $\vec{X}$ is the vector of sampled analog signal, X_i^2 is each sample squared, and n is the number of samples. An operating room is a noisy environment with respect to the recorded signal; therefore, it is crucial to ignore unstable, artifact-containing sessions. Misleading RMS values that result from sources such as neuronal injury potential[17] and other external artifacts were removed using a two-step signal stability test. First, recorded sessions with maximum amplitudes exceeding 300 μV were rejected. This filtered out most external-artifact–contaminated signals. Second, an ANOVA was used to compare the RMS values of 20 millisecond nonoverlapped windows of the signal from the first and last 2 seconds of the signal. The ANOVA was used to evaluate whether they originated from the same population. Recorded sessions displaying significant differences ($P < 0.005$) were considered to be nonstable and were rejected.

RMS values change with the electrode properties and other external drives related to the operating room; therefore, it is crucial to normalize the RMS to comparable

values. Thus, each session's RMS in a trajectory was divided by the mean RMS of the first five stable sessions in the same trajectory. This normalized RMS (NRMS) was found to be a good measure as it reflects the relative change in the total power of the signal, which elevates dramatically entering the STN (Fig. 1). The other parameter that we used is the estimated distance to target (EDT) as a means of integrating the information acquired from the preoperative imaging, with a μm resolution. As the trajectory planning phase predicts the center of STN, the EDT represents the estimated distance from the current electrode tip to that point. All trajectories were initialized 10 mm above the expected center of target and terminated at a variable distance after the neurophysiologist decided STN exit had occurred.

Training Set Bayesian Probability Calculations

Bayesian inference describes how the probability of an event X changes from a prior p(X) before we observe anything to a posterior p(X|Y) once we have observed event Y. Of course, a meaningful change in our prior belief will occur only if X and Y are dependent events, otherwise observing Y will tell us nothing about X, and p(X|Y) = p(X). The general Bayes equation states that (Eq. 2)

$$p(X|Y) = \frac{p(Y|X)*p(X)}{p(Y)} \qquad (2)$$

Each part of Bayes' theorem has a conventional name, which will be used throughout this article. p(X|Y) is

called the posterior probability, i.e., the probability of event X after observing the evidence. p(X) is called the prior probability, which is the initial belief about the tendency of event X. p(Y|X) is called the likelihood probability and is the probability that the evidence will be observed, given X. p(Y) is called the normalizing constant, which is the sum over all X of p(Y|X). With this terminology, the theorem may be paraphrased as

$$Posterior = \frac{Likelihood*Prior}{Normalizing\ Constant}$$

In order to calculate the unknown posterior probabilities, in this case, being in one of the locations given the NRMS-EDT pair, p(Location|(NRMS,EDT)), it was first necessary to calculate the likelihood probability. The likelihood probability here is the tendency to obtain NRMS-EDT pair values in a certain location (pre-, within, or post-STN), p((NRMS,EDT)|Location). To calculate the likelihood probability for each of the three locations, the following steps were followed. One, calculate the sessions' RMS value using Equation 1. Two, normalize each RMS value to the mean RMS value of the first five stable sessions in its trajectory. Three, divide all sessions of all trajectories into three location groups according to the neurophysiologist's decisions. Four, use each group's NRMS-EDT population values to calculate its two-dimensional histogram and divide by the total number of pairs in the group to obtain probabilities.

Since NRMS and EDT are continuous parameters, the values were discretized to obtain meaningful probabilities. NRMS bins ranged from 0 to 7, with a bin size of 0.2. EDT bins ranged from 10 to −6 mm, with a bin size of 1 mm. To overcome noisy data, a narrow two-dimensional smoothing Gaussian filter was used. The filter's standard deviations were 0.5 mm and 0.1 for the EDT and NRMS, respectively (equal to half the bin sizes of EDT and NRMS). The Bayesian prior probability p(Location) represents our prior knowledge regarding the probability of being in each of the locations. To avoid creating a bias toward one of the locations, it was set to 1/3 for each of the three locations. The normalizing constant p((NRMS, EDT)), was set to the sum of the locations conditions as $\sum_{i \in (Locations)} P(NRMS,EDT)_i$. With the smoothed likelihood probabilities, the normalization constant, and the equal prior probabilities, the Bayesian posterior probabilities for each location, p(Location|(NRMS, EDT)) could be calculated according to Bayes's equation (Eq. 2). Note that if an EDT-NRMS pair is not encountered in any of the locations, it will yield a zero posterior probability in the three locations.
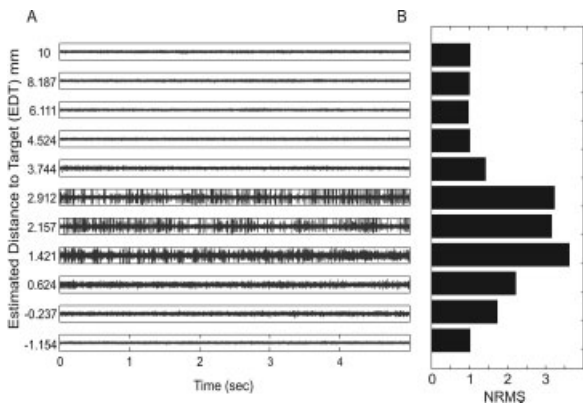

FIG. 1. Sample of signal traces recorded at various depths (in descending order) along a trajectory with their corresponding NRMS values. **A:** Five seconds of raw signal traces presented in decreasing values of EDT. The STN neuronal activity is clearly visible. Y-axis range is 300 μV. **B:** The corresponding NRMS values of the traces in A. Each bar represents the NRMS of the trace on its left. NRMS values increase dramatically when entering the STN and decrease gradually toward its ventral exit.

Method Evaluation

A bootstrapping technique was used to evaluate the accuracy of the results. Each of the 46 trajectories was evaluated with the other 45 trajectories used as a training set for building the Bayesian posterior probability. The following procedure was followed for each evaluated trajectory. One, the posterior probabilities were calculated using the other 45 trajectories. Two, unstable sessions were rejected using the stability test. Three, NRMS was calculated for each stable session. Four, the posterior probabilities for being in each of the locations given the NRMS-EDT pairs were found. Five, the STN entry point was defined as the most dorsal point at which the posterior probability to be within the STN was higher than being prior to it. The STN exit point was taken as the most ventral point at which the posterior probability to be within the STN was still higher than being beyond it. Six, the results were compared to the expert neurophysiologist's decisions by calculating the absolute difference between the expert's STN entry and exit points decisions, and those of our method. We also calculated the deviation from the center of STN defined by the expert and our method, calculated as the central point between the entry and exit points.

Software

Data analysis was carried out on custom software using MATLAB V7 (Mathworks, Natick, MA). The software used in this article can be found online.

RESULTS

Data were recorded from 27 patients undergoing unilateral and bilateral DBS surgery; a total of 46 trajectories were analyzed, of which only 1 originated from unilateral surgery. Another 10 trajectories were omitted due to technical recording problems. On successful trajectories where the STN was recognized by the neurophysiologist, the RMS was distinctively elevated in congruence with the neurophysiologist's STN entry decision (Fig. 2A). On the expert's STN exit point decision RMS values fell, but less sharply than the entry point. On nonsuccessful trajectories, when the neurophysiologist did not recognize the STN activity, RMS values tended to remain low and flat (Fig. 2B). The neurophysiologist's MER-guided targeting moved the center of the STN, as compared to the preoperative imaging targeting, by 1.0 ± 0.72 mm (range, 0.01–3.25 mm).

Bayesian Likelihood and Posterior Probabilities

The raw likelihood probabilities of obtaining an NRMS-EDT pair in each location showed distinctively different results across locations (Fig. 3, A1–A3). For the
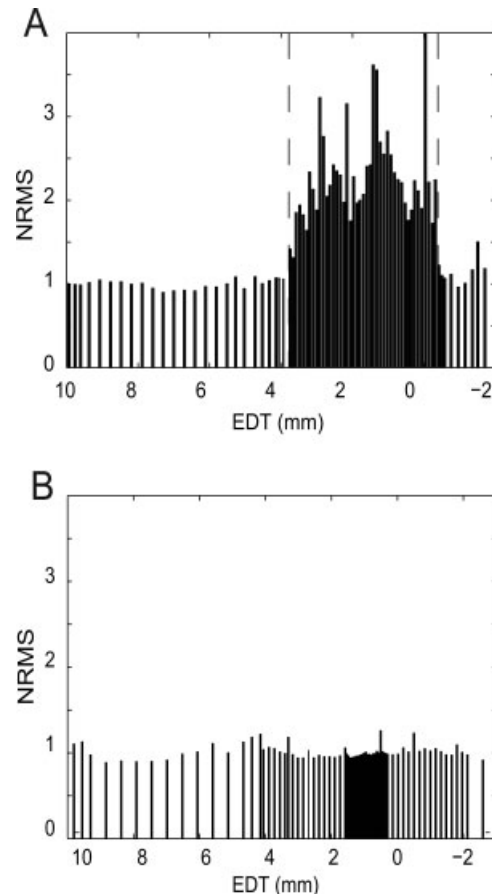

FIG. 2. NRMS values in two sample trajectories. Each line represents the NRMS calculated during one recording session at a certain EDT. Different line densities are caused by differences in electrode advancement steps. **A:** A successful trajectory. Dashed lines indicate the neurophysiologist's decision of entry and exit to the STN. **B:** An unsuccessful trajectory. The NRMS values remain flat, with no significant elevation in NRMS values.

pre-STN location, the highest probabilities occupied the area of high EDT, with narrow NRMS values around 1 (Fig. 3, A1). Within the STN, the highest probabilities tended to occupy the area around -1 EDT, with high NRMS mostly above 1.5 (Fig. 3, A2). Post-STN location high probabilities occupied the lower EDT and a generally wide range of NRMS (Fig. 3, A3). Smoothing the three raw likelihood probabilities with a narrow two-dimensional Gaussian filter created the three smoothed likelihood probabilities (Fig. 3, B1–B3). The smoothed probabilities retain the characteristics of the raw probabilities described above. Using equal prior probabilities caused the posterior probabilities of the three locations to be influenced solely by the likelihood probabilities. Pre-STN posterior high probabilities were mainly in the low NRMS and high (above 0) EDT (Fig. 3, C1). Within-STN high probabilities formed a ball-like shape, which
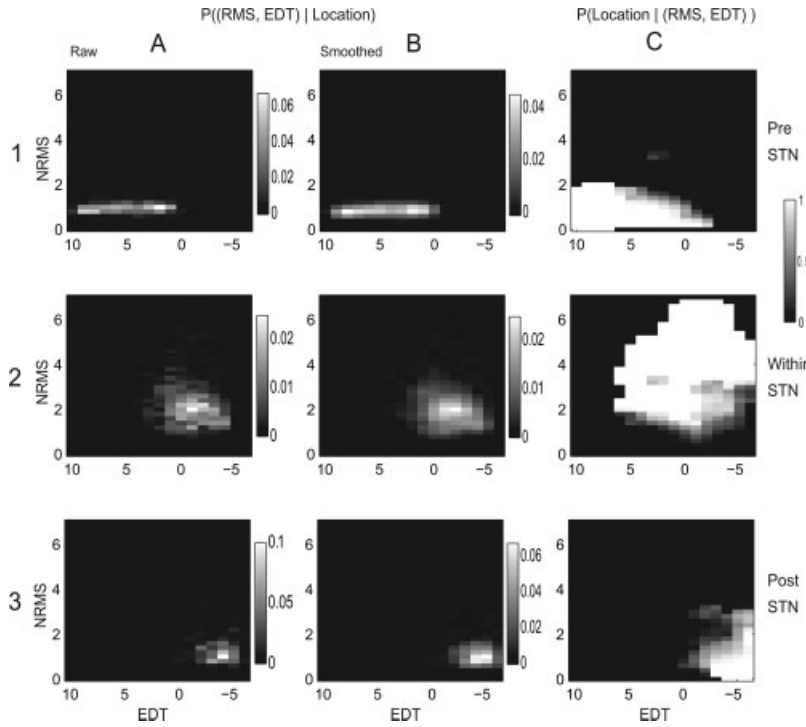
FIG. 3. Posterior probabilities calculation. **A:** The likelihood probability for NRMS and EDT bins for each of the three locations. **B:** The likelihood probability after smoothing with a narrow 2D Gaussian filter (SD of 0.5 mm for EDT and 0.1 for NRMS). **C:** The posterior probability for each location.

centered at high NRMS of ~4 and EDT of −1 (Fig. 3, C2). Post-STN high probabilities were mainly in the low EDT (less than 0) and low NRMS values (Fig. 3, C3).

Technique Evaluation

A bootstrapping technique was used for all the trajectories. Figure 4 shows two of these trajectories, the expert's borders decision and the method's predictions. The quality of the method was assessed by measuring the distance between the expert's decisions and the method's prediction separately for the entry and exit points of the STN. The entry to the STN was better predicted, with an error of 0.18 ± 0.84 mm, whereas the exit of the STN was also predicted quite successfully, but with less accuracy: 0.50 ± 0.59 mm. This border evaluation led to an error of 0.30 ± 0.28 mm in the prediction of the center of the STN compared to the expert's STN center.

DISCUSSION

Choosing the normalized RMS as the prime parameter for evaluating STN borders was found to be highly predictive. Several parameters contributed to this success: the high neuronal density within the STN[18] combined with its high sustained spontaneous activity[2,13] led to a sharp increase in the overall power of the signal detected by the electrode within the STN. The generally low density/low activity in its surrounding structures accentuated this feature. Adding the EDT parameter

helped overcome occasional rare high RMS values that were encountered outside the STN due to cell injuries by the moving electrode, or normal cellular activity of other structures. These results show that by using Bayesian inference on these two simple measures, over a short (5 seconds) recording duration, the entry into and exit from the STN can be predicted. This simple method can help the surgical team assess in real-time the location of the STN in the trajectory. Moreover, this method, which uses low computational resources and relies on readily available electrodes and equipment, can be easily introduced to guiding systems currently in clinical use. The considerable differences between the MER-guided expert decisions and the preoperative imaging target highlight the importance of MER in target localization.

Although this method relies on simple measures such as the NRMS and EDT, care should be taken when applying it in real-time intraoperative scenarios. To reduce the influence of electrode movement on the computed NRMS, it is recommended to wait 2 seconds before recording. Another source of misleading information regarding the NRMS comes from neuronal injury potentials,[17] produced when a neuron is damaged by the electrode. These cell injuries are characterized by high spike discharge that gradually fades, sometime over periods of more than 2 seconds. This well-known phenomenon gives rise to a high abnormal NRMS value. To
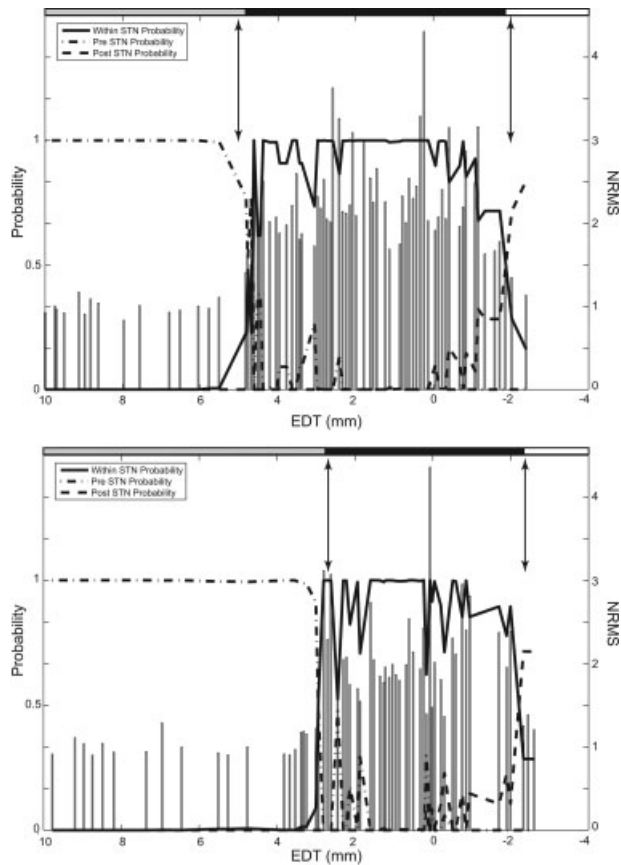
FIG. 4. Location evaluations of two trajectories. Given a trajectory, the posterior probability of being in each of the locations is calculated. Arrows indicate expert's STN entry and exit points decision. The maximum likelihood estimation (MLE), which in this case is the highest probability of the three locations (gray, black, and white color encoding for pre, within, and post-STN, respectively) is shown above panels. The expert's and our system's decisions closely coincide.

overcome this and other artifacts that may lead to erroneous location decisions, we applied a signal stability test that rejects unstable recorded sessions. While this method eliminated noisy data, it introduced some entry and exit point prediction errors when the sessions defined by the expert as entry/exit points were unstable and therefore rejected and could not be assessed. We also encountered trajectories where in postoperative data analysis, the expert's decisions were closer to the system's borders decisions than to his intraoperative decisions. Despite these findings, the expert's decisions were clearly adequate as a teacher for the system.

The method described in this article varies in its capability to predict the entry and exit of STN. Whereas the entry to the STN was usually clear and characterized by a distinguishable rise of the RMS, the exit of the STN was harder to predict in some of the trajectories. This is

primarily due to the anatomical and physiological differences between the structures before and after the STN. Along the trajectories, the structures preceding the STN are usually the thalamus, the areas of the zona incerta, and/or the field of Forel, all of which produce low NRMS values. Ventral to the STN lies the substantia nigra pars reticulata (SNr). Although histologically and neurophysiologically distinct from the STN,[2,19,20] the transition between the two nuclei was not always clear either to the expert or to our system. One factor leading to the small differences between STN and post-STN RMS values was a notable decrease in the magnitude of the NRMS within the STN while traversing toward its ventral part, which was found in some of the trajectories (Fig. 5A). This general decline of NRMS created further difficulties in
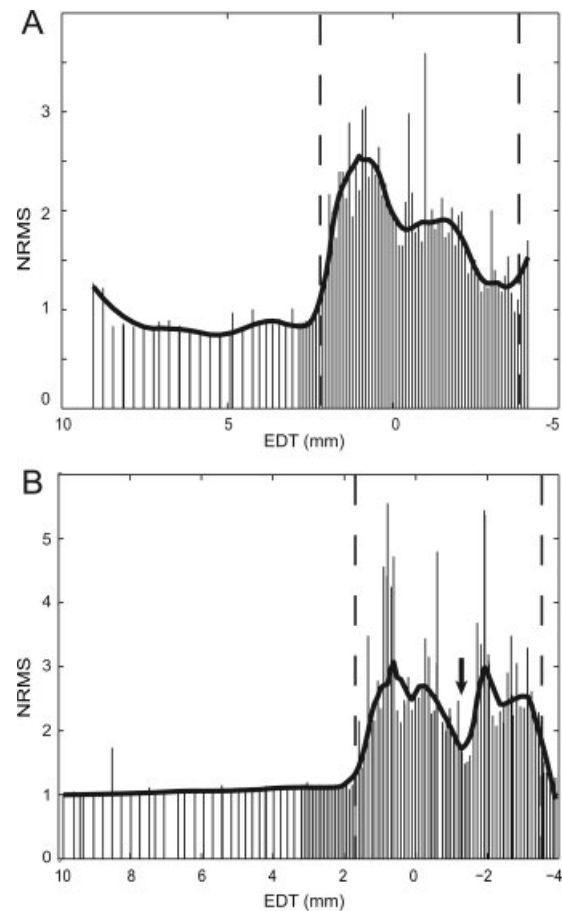

FIG. 5. NRMS changes within the STN. Two phenomena emerged from NRMS analysis of the trajectory sessions. **A:** Whereas some sessions show roughly constant high NRMS values along the STN, some trajectories show a general decrease in NRMS values toward its ventral area. Solid line indicates Gaussian smoothing of the NRMS values; dashed line indicates STN boundaries. **B:** The NRMS dip, a quiet area inside the STN, was encountered along several trajectories. Arrow indicates the dip; solid and dashed lines as in A.

identifying the STN exit point. Another phenomenon that did not contribute to localization, but was nevertheless interesting, was a dip in the RMS values while still within the STN (Fig. 5B) that was found in some trajectories.

An additional advantage of this Bayesian approach is the ease in which additional localizing parameters can be added in the future. Currently, the likelihood probability consists of only two parameters: the NRMS and EDT. Future plans are to include more parameters, such as spectral features of the analog signal, local field potential (LFP),[21] and other "spike sorting free" parameters to the likelihood probability, in order to enhance accuracy. This may aid in detecting the STN ventral border near the SNr, where the NRMS transition between nuclei is less clear. The two most notable advantages of this method are its independence of online detection and sorting of spiking activity and the short recording time needed for location analysis. Online spike sorting is a pitfall for most other STN localization techniques. Whereas neuronal spike characteristics (i.e., firing rate, burstiness, oscillation, and spike shape) of the STN and other structures have been well studied[7–9] and do enhance STN localization, it is still computationally impractical to calculate in a real-time intraoperative scenario. In contrast, the NRMS is low-cost computationally and can be calculated in real time with ease. The same holds true for the posterior probability calculation. A further obvious phase would be to automate the whole targeting procedure. With the simplicity of the NRMS calculation and the short periods of time needed to record in each depth, an automated procedure that advances the electrode, records the signal, evaluates location, and advances the electrode to the next depth is simple to implement. The outcomes of our procedure of reduced surgery time, together with finer precision of STN localization, may reduce the risk of postoperative complications and enhance surgery clinical effects by better electrode positioning.

REFERENCES

1. Limousin P, Pollak P, Benazzouz A, et al. Bilateral subthalamic nucleus stimulation for severe Parkinson's disease. Mov Disord 1995;10:672–674.

2. Hutchison WD, Allan RJ, Opitz H, et al. Neurophysiological identification of the subthalamic nucleus in surgery for Parkinson's disease. Ann Neurol 1998;44:622–628.

3. Starr PA. Placement of deep brain stimulators into the subthalamic nucleus or Globus pallidus internus: technical approach. Stereotact Funct Neurosurg 2002;79:118–145.

4. Anderson VC, Burchiel KJ, Hogarth P, et al. Pallidal vs subthalamic nucleus deep brain stimulation in Parkinson disease. Arch Neurol 2005;62:554–560.

5. Israel Z, Burchiel KJ. Microelectrode Recording in Movement Disorder Surgery. Stuttgart: Thieme; 2004.

6. Cuny E, Guehl D, Burbaud P, et al. Lack of agreement between direct magnetic resonance imaging and statistical determination of a subthalamic target: the role of electrophysiological guidance. J Neurosurg 2002;97:591–597.

7. Benazzouz A, Breit S, Koudsie A, et al. Intraoperative microrecordings of the subthalamic nucleus in Parkinson's disease. Mov Disord 2002;17(Suppl. 3):S145–S149.

8. Sterio D, Zonenshayn M, Mogilner AY, et al. Neurophysiological refinement of subthalamic nucleus targeting. Neurosurgery 2002; 50:58–67.

9. Pesenti A, Rohr M, Egidi M, et al. The subthalamic nucleus in Parkinson's disease: power spectral density analysis of neural intraoperative signals. Neurol Sci 2004;24:367–374.

10. Santiago RA, McNames J, Burchiel K, et al. Developments in understanding neuronal spike trains and functional specializations in brain regions. Neural Netw 2003;16:601–607.

11. Falkenberg JH, McNames J, Burchiel K. Statistical methods of analysis and visualization of extracellular microelectrode recording. Cancun, Mexico: Proccedings of the Annual International Conference of the IEEE Engineering in Medicine and Biology; 2003. p 2515–2518.

12. Pralong E, Villemure JG, Bloch J, et al. Quality index for the quantification of the information recorded along standard microelectrode tracks to the subthalamic nucleus in parkinsonian patients. Neurophysiol Clin 2004;34:209–215.

13. Wichmann T, Bergman H, DeLong MR. The primate subthalamic nucleus: I, functional properties in intact animals. J Neurophysiol 1994;72:494–506.

14. Rodriguez-Oroz MC, Rodriguez M, Guridi J, et al. The subthalamic nucleus in Parkinson's disease: somatotopic organization and physiological characteristics. Brain 2001;124:1777–1790.

15. Bevan MD, Magill PJ, Terman D, et al. Move to the rhythm: oscillations in the subthalamic nucleus-external globus pallidus network. Trends Neurosci 2002;25:525–531.

16. Lewicki MS. A review of methods for spike sorting: the detection and classification of neural action potentials. Network 1998;9: R53–R78.

17. Cranefield PF, Eyster JAE, Gilson WE. Electrical characteristics of injury potentials. Am J Physiol 1951;167:450–456.

18. Hardman CD, Henderson JM, Finkelstein DI, et al. Comparison of the basal ganglia in rats, marmosets, macaques, baboons, and humans: volume and neuronal number for the output, internal relay, and striatal modulating nuclei. J Comp Neurol 2002;445: 238–255.

19. DeLong MR, Crutcher MD, Georgopoulos AP. Relations between movement and single cell discharge in the substantia nigra of the behaving monkey. J Neurosci 1983;3:1599–1606.

20. Wichmann T, Bergman H, Starr PA, et al. Comparison of MPTP-induced changes in spontaneous neuronal discharge in the internal pallidal segment and in the substantia nigra pars reticulata in primates. Exp Brain Res 1999;125:397–409.

21. Chen CC, Pogosyan A, Zrinzo LU, et al. Intra-operative recordings of local field potentials can help localize the subthalamic nucleus in Parkinson's disease surgery. Exp Neurol 2006;198:214–221.